Figure S1. Related to Figure 1. CRISPR screen hits and molecular profiles.
(A) Gene set enrichment analysis (GSEA) shows the association between top hit genes and ribosomal genes in SUM159 cells.
(B) Top co-dependencies of *BRD4* in TNBC in DepMap. Genes are ranked by co-dependency score between *BRD4* and every other gene. Co-dependent and anti-dependent hits (cutoff = 0.3) are marked in orange and cyan, respectively.
(C) Top hit genes between CRISPR screen of untreated vs. JQ1-treated SUM149/SUM159 (x-axis) and co-dependencies of *BRD4* in TNBC in DepMap (y-axis). x-axis: log10(p-values); y-axis: co-dependency score. Significant resistance and synthetic lethal hits (p-value cutoff: 0.001, co-dependency score cutoff: 0.3) are marked in red and blue, respectively.
(D) Top process networks enriched in JQ1 synergistic and resistance CRISPR screen hits in SUM149 and SUM149R cells.
(E) Mutated genes detected in BBDI-resistant but not in parental SUM149 and SUM159 cells. Red highlight indicates mutated genes detected in both resistant cell lines.
(F) DNA methylation of CpG islands in SUM149 and SUM159 parental and JQ1-resistant cells. The box indicates the IQR, the line inside the box shows the median, and whiskers show the locations of 1.5 x IQR above the third quartile and 1.5 x IQR below the first quartile.
(G) Correlation plot between differentially methylated and expressed genes in the indicated cell lines.
(H) Heatmap of histone mass spectrometry data in the indicated cell lines with and without JQ1 treatment.
(I) Heatmap of top process networks enriched in genes that are upregulated (red) or downregulated (blue) by RNA-seq in treated vs. untreated parental and BBDI-resistant cell lines and in untreated and treated resistant vs. parental cell lines.

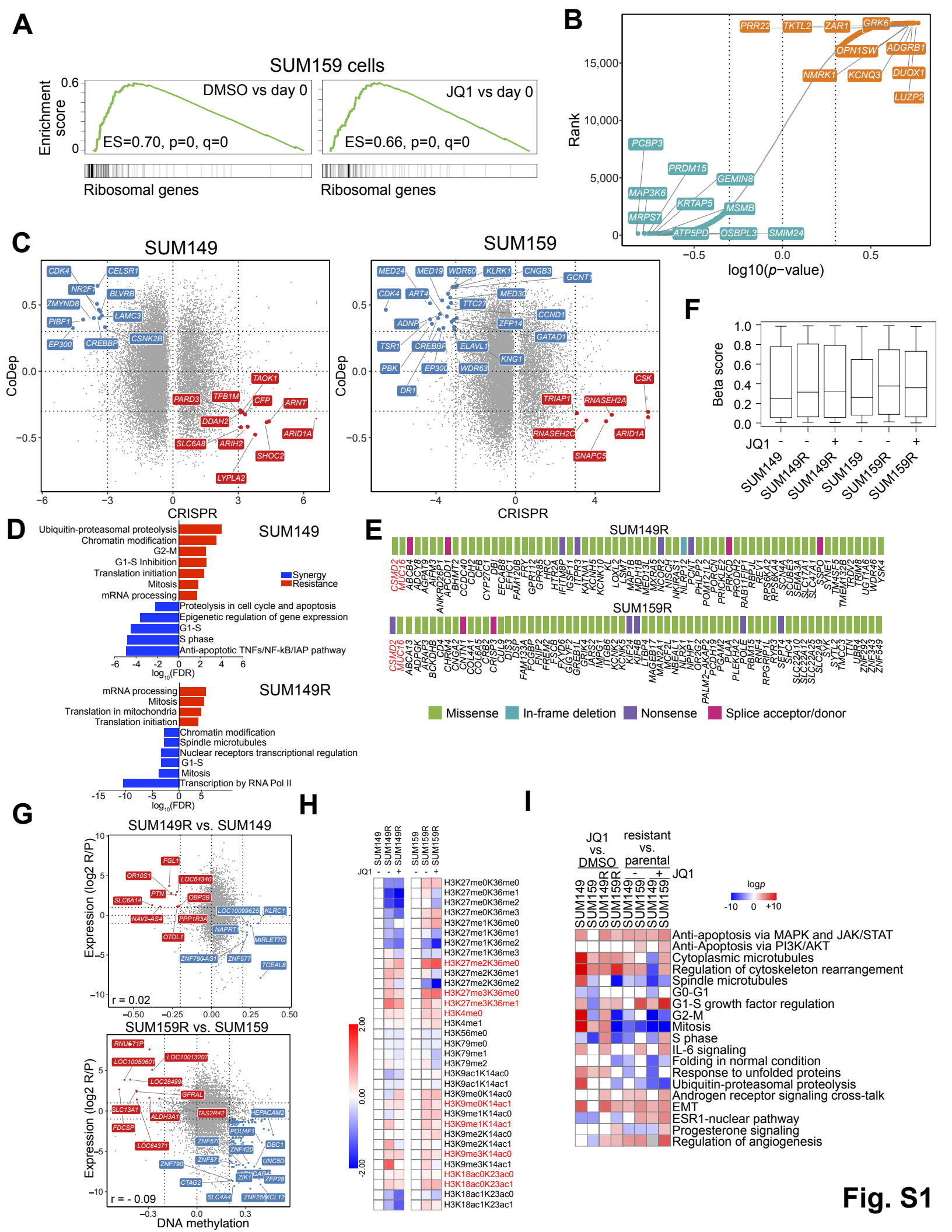
A
SUM159 cells
Enrichment score
DMSO vs day 0
ES=0.70, p=0, q=0
JQ1 vs day 0
ES=0.66, p=0, q=0
Ribosomal genes
Ribosomal genes
B
Rank
log10(p−value)
PRR22
TKTL2
ZAR1
GRK6
OPN1SW
ADGRB1
NMRK1
KCNQ3
DUOX1
LUZP2
PCBP3
PRDM15
GEMIN8
MAP3K6
KRTAP5
MSMB
MRPS7
ATP5PD
OSBPL3
SMIM24
C
SUM149
SUM159
CoDep
CRISPR
CDK4
CELSR1
NR2F1
BLVRB
ZMYND8
LAMC3
PIBF1
CSNK2B
EP300
CREBBP
TAOK1
PARD3
TFB1M
CFP
ARNT
DDAH2
ARID1A
SLC6A8
ARIH2
SHOC2
LYPLA2
MED24
MED19
WDR60
KLRK1
CNGB3
GCNT1
CDK4
ART4
MED30
TTC27
CCND1
ADNP
ZFP14
GATAD1
TSR1
CREBBP
ELAVL1
KNG1
PBK
EP300
WDR63
DR1
CSK
TRIAP1
RNASEH2A
RNASEH2C
ARID1A
SNAPC5
F
Beta score
JQ1
SUM149
SUM149R
SUM149R
SUM159
SUM159R
SUM159R
D
SUM149
Ubiquitin-proteasomal proteolysis
Chromatin modification
G2-M
G1-S Inhibition
Translation initiation
Mitosis
mRNA processing
Synergy
Resistance
Proteolysis in cell cycle and apoptosis
Epigenetic regulation of gene expression
G1-S
S phase
Anti-apoptotic TNFs/NF-kB/IAP pathway
log10(FDR)
SUM149R
mRNA processing
Mitosis
Translation in mitochondria
Translation initiation
Chromatin modification
Spindle microtubules
Nuclear receptors transcriptional regulation
G1-S
Mitosis
Transcription by RNA Pol II
log10(FDR)
E
SUM149R
SUM159R
CSMD2
MUC16
Missense
In-frame deletion
Nonsense
Splice acceptor/donor
G
SUM149R vs. SUM149
Expression (log2 R/P)
r = 0.02
SUM159R vs. SUM159
r = - 0.09
DNA methylation
H
SUM149
SUM149R
SUM149R
SUM159
SUM159R
SUM159R
JQ1
H3K27me0K36me0
H3K27me0K36me1
H3K27me0K36me2
H3K27me0K36me3
H3K27me1K36me0
H3K27me1K36me1
H3K27me1K36me2
H3K27me1K36me3
H3K27me2K36me0
H3K27me2K36me1
H3K27me2K36me2
H3K27me3K36me0
H3K27me3K36me1
H3K4me0
H3K4me1
H3K56me0
H3K79me0
H3K79me1
H3K79me2
H3K9ac1K14ac0
H3K9ac1K14ac1
H3K9me0K14ac0
H3K9me0K14ac1
H3K9me1K14ac0
H3K9me1K14ac1
H3K9me2K14ac0
H3K9me2K14ac1
H3K9me3K14ac0
H3K9me3K14ac1
H3K18ac0K23ac0
H3K18ac0K23ac1
H3K18ac1K23ac0
H3K18ac1K23ac1
I
JQ1 vs. DMSO
resistant vs. parental
JQ1
SUM149
SUM159
SUM149R
SUM159R
SUM149
SUM159
SUM149
SUM159
logp
Anti-apoptosis via MAPK and JAK/STAT
Anti-Apoptosis via PI3K/AKT
Cytoplasmic microtubules
Regulation of cytoskeleton rearrangement
Spindle microtubules
G0-G1
G1-S growth factor regulation
G2-M
Mitosis
S phase
IL-6 signaling
Folding in normal condition
Response to unfolded proteins
Ubiquitin-proteasomal proteolysis
Androgen receptor signaling cross-talk
EMT
ESR1-nuclear pathway
Progesterone signaling
Regulation of angiogenesis

Fig. S1

Figure S2. Related to Figure 1. CRISPR screen hits and molecular profiles.
(A) Heatmap of proteins identified in RPPA data by k-means clustering (*k* = 12). (B) Heatmap of top differentially regulated pathways in RPPA data.
(C) Heatmap of proteins from RPPA assay highly expressed exclusively in SUM159R cells (cluster 2), SUM149R cells (clusters 6, 7, and 9) and in both SUM149R and SUM159R cells (cluster 12).
(D) Average expression of all cell cycle proteins by RPPA in SUM149 and SUM159 parental and resistant cells with or without JQ1 treatment.
(E) Heatmap of CRISPR screen hits and their gene expression changes in SUM149 and SUM149R cells. Hits with gene expression fold changes greater than 2 in any paired comparison are shown.
(F) Heatmap of CRISPR screen hits and their gene expression changes in SUM159 and SUM159R cells. Hits with gene expression fold changes greater than 2 in any paired comparison are shown.
(G) Heatmap of BRD4 RIME data in SUM159 and SUM159R cells with and without JQ1 treatment, compared to untreated SUM159. Grey shows the missing data.
(H) Immunoblot analysis of total cell lysates (input) and BRD4 immunoprecipitates (IP) from SUM149 and SUM149R cells with and without 3h JQ1 (2 μM) treatment.
(I) Top process networks enriched in proteins bound to BRD4, comparing JQ1 vs. DMSO treatment in SUM149 and SUM149R and comparing SUM149R vs. SUM149 cells during JQ1 and DMSO treatment.
(J) Heatmap of top CRISPR screen hits and their BRD4-binding changes in SUM159 and SUM159R cells in JQ1 compared to DMSO and in SUM159R compared to SUM159. Red and blue bars represent significant resistant and synthetic lethal hits (p-value < 0.001) in the CRISPR screen of SUM159 cells, respectively.

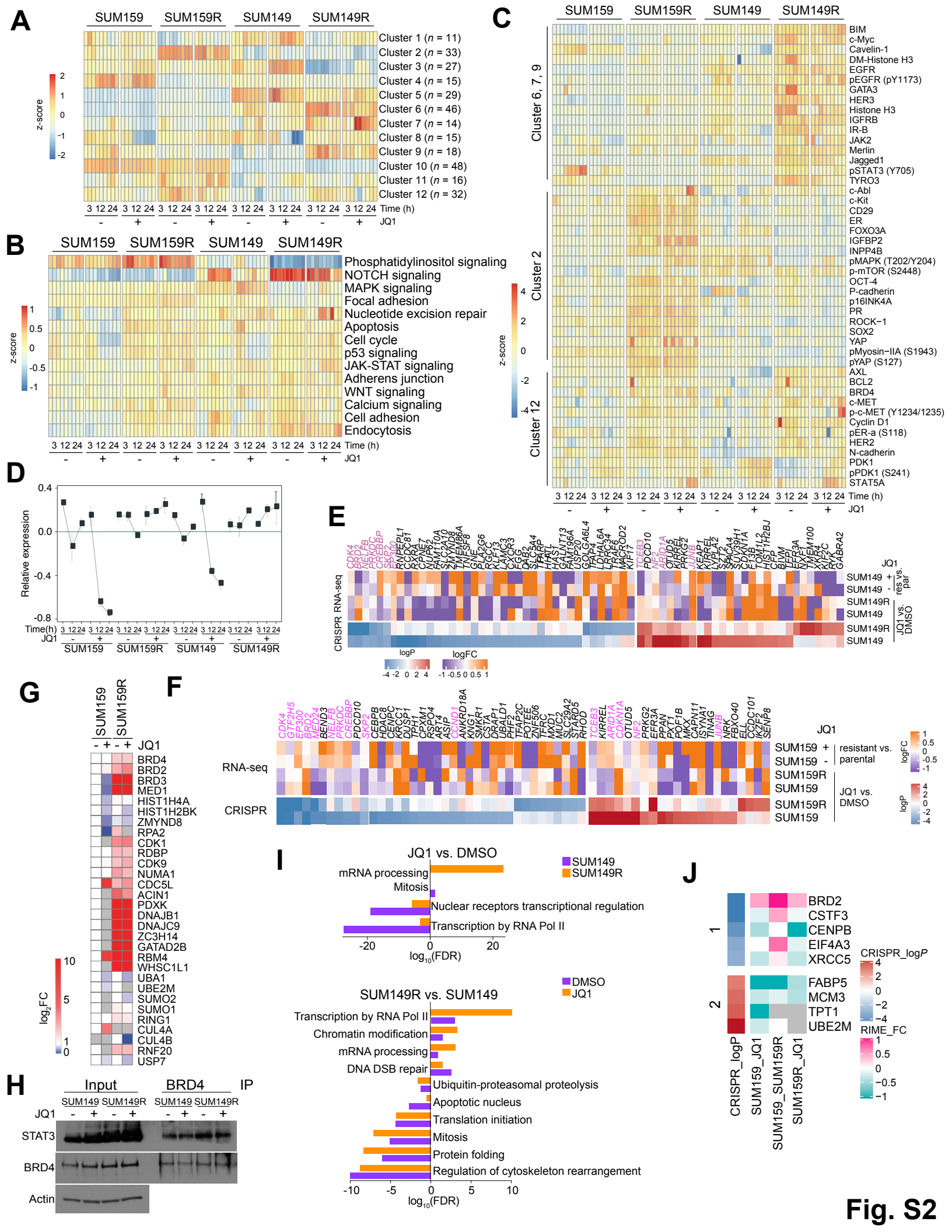
A
SUM159
SUM159R
SUM149
SUM149R
z-score
Cluster 1 (n = 11)
Cluster 2 (n = 33)
Cluster 3 (n = 27)
Cluster 4 (n = 15)
Cluster 5 (n = 29)
Cluster 6 (n = 46)
Cluster 7 (n = 14)
Cluster 8 (n = 15)
Cluster 9 (n = 18)
Cluster 10 (n = 48)
Cluster 11 (n = 16)
Cluster 12 (n = 32)
Time (h)
JQ1
B
Phosphatidylinositol signaling
NOTCH signaling
MAPK signaling
Focal adhesion
Nucleotide excision repair
Apoptosis
Cell cycle
p53 signaling
JAK-STAT signaling
Adherens junction
WNT signaling
Calcium signaling
Cell adhesion
Endocytosis
C
Cluster 6, 7, 9
Cluster 2
Cluster 12
BIM
c-Myc
Cavelin-1
DM-Histone H3
EGFR
pEGFR (pY1173)
GATA3
HER3
Histone H3
IGFRB
IR-B
JAK2
Merlin
Jagged1
pSTAT3 (Y705)
TYRO3
c-Abl
c-Kit
CD29
ER
FOXO3A
IGFBP2
INPP4B
pMAPK (T202/Y204)
p-mTOR (S2448)
OCT-4
P-cadherin
p16INK4A
PR
ROCK−1
SOX2
YAP
pMyosin−IIA (S1943)
pYAP (S127)
AXL
BCL2
BRD4
c-MET
p-c-MET (Y1234/1235)
Cyclin D1
pER-a (S118)
HER2
N-cadherin
PDK1
pPDK1 (S241)
STAT5A
D
Relative expression
Time(h)
JQ1
SUM159
SUM159R
SUM149
SUM149R
E
RNA-seq
CRISPR
JQ1
SUM149 + res. vs. par
SUM149 - res. vs. par
SUM149R JQ1 vs. DMSO
SUM149 JQ1 vs. DMSO
logP
logFC
F
RNA-seq
CRISPR
JQ1
SUM159 + resistant vs. parental
SUM159 - resistant vs. parental
SUM159R JQ1 vs. DMSO
SUM159 JQ1 vs. DMSO
SUM159R JQ1 vs. DMSO
SUM159 JQ1 vs. DMSO
logFC
logP
G
SUM159
SUM159R
JQ1
log2FC
BRD4
BRD2
BRD3
MED1
HIST1H4A
HIST1H2BK
ZMYND8
RPA2
CDK1
RDBP
CDK9
NUMA1
CDC5L
ACIN1
PDXK
DNAJB1
DNAJC9
ZC3H14
GATAD2B
RBM4
WHSC1L1
UBA1
UBE2M
SUMO2
SUMO1
RING1
CUL4A
CUL4B
RNF20
USP7
H
Input
BRD4
IP
SUM149
SUM149R
JQ1
STAT3
BRD4
Actin
I
JQ1 vs. DMSO
SUM149
SUM149R
mRNA processing
Mitosis
Nuclear receptors transcriptional regulation
Transcription by RNA Pol II
log10(FDR)
SUM149R vs. SUM149
DMSO
JQ1
Transcription by RNA Pol II
Chromatin modification
mRNA processing
DNA DSB repair
Ubiquitin-proteasomal proteolysis
Apoptotic nucleus
Translation initiation
Mitosis
Protein folding
Regulation of cytoskeleton rearrangement
log10(FDR)
J
BRD2
CSTF3
CENPB
EIF4A3
XRCC5
FABP5
MCM3
TPT1
UBE2M
CRISPR_logP
SUM159_JQ1
SUM159R_JQ1
CRISPR_logP
RIME_FC

Fig. S2

Figure S3. Related to Figures 1 and 2. Validation of CRISPR data and Small Molecule Inhibitor screens.

(A) Normalized read counts for all sgRNAs in the CRISPR screen targeting *BRD2* and *CDK4* in SUM159R and SUM149R cells and targeting *BRD7* in SUM159 cells, before and after 5 passages of selection. Each color represents a unique gRNA. The sequence for each gRNA is indicated. gRNAs selected for further validation are marked as g1 and g2.

(B) Immunoblot analysis of *CDK4*, *BRD2*, and *BRD7* knockout (KO) single cell clones derived from SUM159 and SUM159R cell lines.

(C) Growth curves of scramble sgRNA, CDK4, BRD2, and BRD7 knockout single cell clones derived from SUM159 and SUM159R cell lines treated with JQ1 at the indicated concentrations.

(D) Immunoblot analysis of endogenous *CDK4* knockout (KO) single cell clones derived from SUM159 cell line expressing a TET-inducible sgRNA-insensitive *CDK4* grown in the presence (+dox) or absence (-dox) of doxycycline.

(E) Growth curves of *CDK4* knockout single cell clones expressing a TET-inducible sgRNA-insensitive *CDK4*, treated with JQ1 at indicated concentrations and grown in the presence (+dox) or absence (-dox) of doxycycline.

(F) Pathways targeted by each compound library.

(G) Dose-response curves for JQ1 in SUM149 and SUM159 parental and JQ1-resistant cells.

(H) The differential drug sensitivity was calculated as the difference between parental and JQ1-resistant cell lines in area under the dose-response curves (AUC) across 10 dilution points after 72 hours of treatment.

(I) Individual dose-response curves for the combination treatments of top hit drugs with JQ1 (2 μM) in SUM149 and SUM149R cells. Statistical analysis of dose-curves was completed in GraphPad Prism 8 (nonlinear regression, variable slope, four parameters, bottom constant equal to 0, top constant equal to 1). LogIC50 values were compared with an extra sum-of-squares F Test.

(J) Immunoblot analysis of the indicated proteins in parental SUM149 and SUM159 and JQ1-resistant SUM149R and SUM159R cell lines following 24 hours treatment with flavopiridol (CDK inhibitor) or barasertib (HDAC inhibitor). The drug concentrations were IC80 values based on IC50 curves (flavopiridol: SUM149 and SUM149R cell lines 1μM, SUM159 0.1 μM and SUM159R 0.2 μM, Barasertib: SUM149 and SUM149R cell lines 1μM, SUM159 and SUM159R cell lines 2 μM).

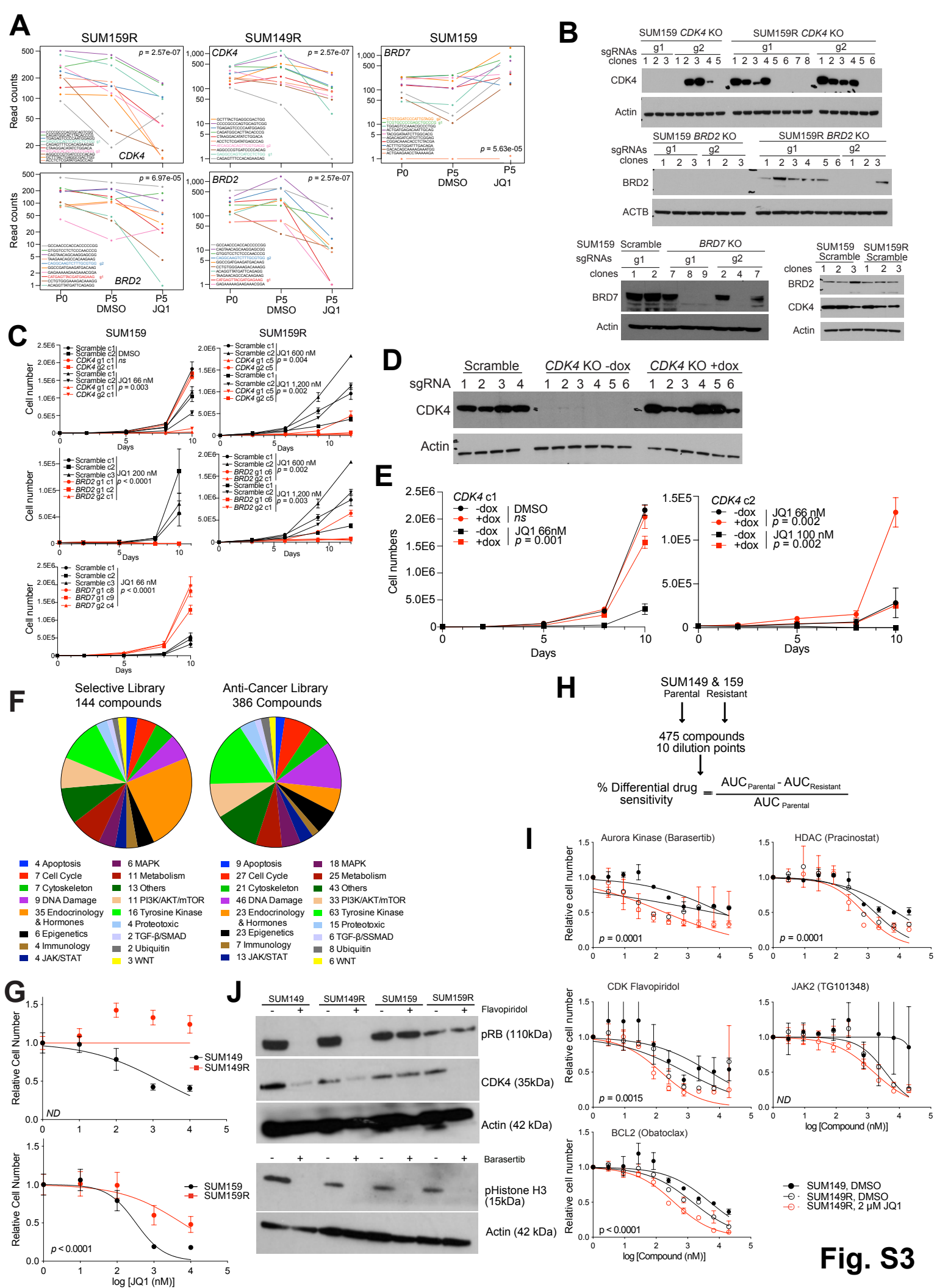
A
SUM159R
SUM149R
SUM159
CDK4
BRD7
BRD2
Read counts
p = 2.57e-07
p = 6.97e-05
p = 5.63e-05
P0
P5 DMSO
P5 JQ1
B
SUM159 CDK4 KO
SUM159R CDK4 KO
sgRNAs
clones
CDK4
Actin
SUM159 BRD2 KO
SUM159R BRD2 KO
BRD2
ACTB
SUM159 Scramble
BRD7 KO
BRD7
SUM159R Scramble
C
SUM159
SUM159R
Cell number
Days
Scramble c1
Scramble c2
CDK4 g1 c1
CDK4 g2 c1
CDK4 g1 c5
CDK4 g2 c5
BRD2 g1 c1
BRD2 g1 c2
BRD2 g2 c1
BRD2 g1 c6
BRD2 g2 c6
BRD7 g1 c8
BRD7 g1 c9
BRD7 g2 c4
DMSO
JQ1 66 nM
JQ1 200 nM
JQ1 600 nM
JQ1 1,200 nM
D
Scramble
CDK4 KO -dox
CDK4 KO +dox
sgRNA
CDK4
Actin
E
CDK4 c1
CDK4 c2
-dox
+dox
DMSO
JQ1 66nM
JQ1 66 nM
JQ1 100 nM
Cell numbers
Days
F
Selective Library
144 compounds
Anti-Cancer Library
386 Compounds
4 Apoptosis
7 Cell Cycle
7 Cytoskeleton
9 DNA Damage
35 Endocrinology & Hormones
6 Epigenetics
4 Immunology
4 JAK/STAT
6 MAPK
11 Metabolism
13 Others
11 PI3K/AKT/mTOR
16 Tyrosine Kinase
4 Proteotoxic
2 TGF-β/SMAD
2 Ubiquitin
3 WNT
9 Apoptosis
27 Cell Cycle
21 Cytoskeleton
46 DNA Damage
23 Endocrinology & Hormones
23 Epigenetics
7 Immunology
13 JAK/STAT
18 MAPK
25 Metabolism
43 Others
33 PI3K/AKT/mTOR
63 Tyrosine Kinase
15 Proteotoxic
6 TGF-β/SSMAD
8 Ubiquitin
6 WNT
H
SUM149 & 159
Parental
Resistant
475 compounds
10 dilution points
% Differential drug sensitivity = AUC Parental - AUC Resistant / AUC Parental
I
Aurora Kinase (Barasertib)
HDAC (Pracinostat)
CDK Flavopiridol
JAK2 (TG101348)
BCL2 (Obatoclax)
Relative cell number
log [Compound (nM)]
p = 0.0001
p = 0.0015
p < 0.0001
ND
SUM149, DMSO
SUM149R, DMSO
SUM149R, 2 μM JQ1
G
Relative Cell Number
SUM149
SUM149R
SUM159
SUM159R
p < 0.0001
log [JQ1 (nM)]
J
SUM149
SUM149R
SUM159
SUM159R
Flavopiridol
pRB (110kDa)
CDK4 (35kDa)
Actin (42 kDa)
Barasertib
pHistone H3 (15kDa)
Actin (42 kDa)

Fig. S3

Figure S4. Related to Figures 3 and 4. Validation of synergy hits and BET6 BET bromodomain protein degrader.

(A) Synergy studies of JQ1 with palbociclib in a panel of TNBC cell lines in culture. Points represent paired values of drug concentrations assessed for synergism. The diagonal line signifies drug additivity. Points above and below the line represent antagonistic and synergistic drug combinations, respectively.

(B) Hematoxylin and eosin staining of SUM149R and SUM159R xenografts from mice treated with various compounds alone or combined with JQ1. Scale bars represent 50 μm.

(C) Immunofluorescence analysis of cleaved caspase-3 in SUM149R xenografts from mice treated with the indicated compounds alone or combined with JQ1. Scale bars show 50 μm.

(D) Immunofluorescence analysis of phospho-STAT3 levels in SUM150R xenografts.

(E) Tumor volumes of xenografts from mice treated with JQ1 and palbociclib alone and in combination. None of the differences were statistically significant.

(F) Hematoxylin and eosin staining of SUM159R xenografts and patient-derived xenografts IDC50 from mice treated with JQ1 and palbociclib, alone and in combination. Scale bars represent 50 μm.

(G) Immunofluorescence analysis of phospho-RB levels in SUM150R xenografts.

(H) Immunoblot analysis of BRD2, BRD4, BRD7, CDK4, CCND1, phospho-RB, and RB in SUM159 and SUM159R cells at different time points after JQ1 (2μM), palbociclib (1μM), and combination treatment.

(I) Chemical structures of JQ1, phthalimide, dBET1, and dBET6.

(J) Immunoblot analysis of BRD4 protein levels in SUM149R cells treated with 250 nM of dBET6.

(K) Heatmap of $\log_2$ fold changes in gene expression after 2 and 6 hours of treatment with 250 nM of dBET6. Expression values were normalized to ERCC spike-ins to allow for cell count normalized quantification.

(L) Immunoblot analysis of RNA polymerase II phosphorylation levels at the indicated time points after treatment with 250 nM of dBET6.

(M) Tumor weights of SUM149R and SUM159R xenografts treated with JQ1 (50 mg/kg, daily) or dBET6 [10 mg/kg, once (qd) or twice (bid) daily].

(N) Hematoxylin-eosin and Ki67 staining of SUM149R and SUM159R xenografts from mice treated with JQ1 or dBET6. Scale bars represent 50 μm.

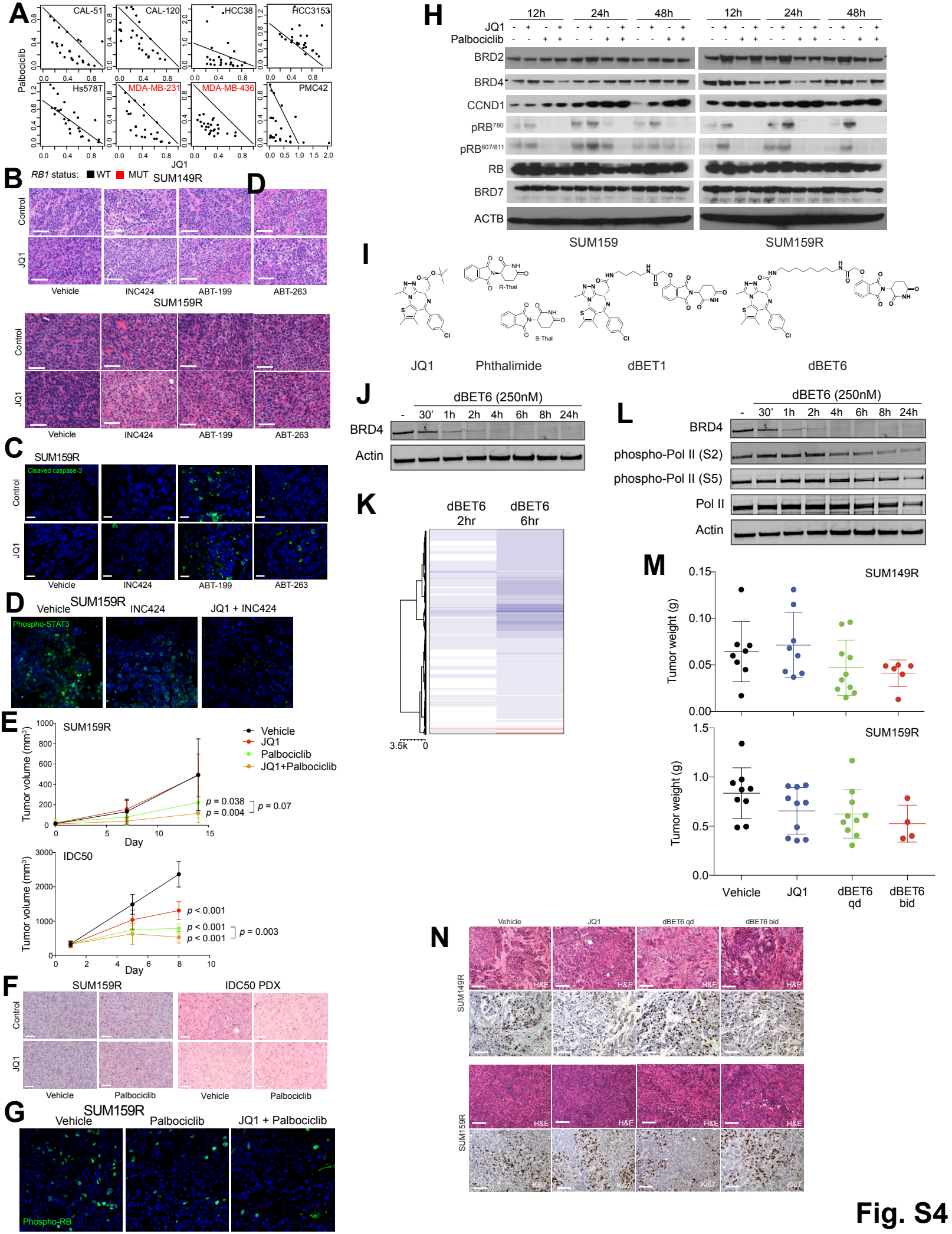
A
CAL-51
CAL-120
HCC38
HCC3153
Hs578T
MDA-MB-231
MDA-MB-436
PMC42
Palbociclib
JQ1
B
RB1 status: WT MUT
SUM149R
Control
JQ1
Vehicle
INC424
ABT-199
ABT-263
SUM159R
C
SUM159R
Cleaved caspase-3
D
SUM159R
Vehicle
INC424
JQ1 + INC424
Phospho-STAT3
E
SUM159R
Vehicle
JQ1
Palbociclib
JQ1+Palbociclib
Tumor volume (mm3)
Day
p = 0.038
p = 0.004
p = 0.07
IDC50
p < 0.001
p < 0.001
p < 0.001
p = 0.003
F
SUM159R
IDC50 PDX
G
SUM159R
Vehicle
Palbociclib
JQ1 + Palbociclib
Phospho-RB
H
12h
24h
48h
JQ1
Palbociclib
BRD2
BRD4
CCND1
pRB780
pRB807/811
RB
BRD7
ACTB
SUM159
SUM159R
I
R-Thal
S-Thal
JQ1
Phthalimide
dBET1
dBET6
J
dBET6 (250nM)
- 30' 1h 2h 4h 6h 8h 24h
BRD4
Actin
K
dBET6 2hr
dBET6 6hr
3.5k
0
L
dBET6 (250nM)
BRD4
phospho-Pol II (S2)
phospho-Pol II (S5)
Pol II
Actin
M
SUM149R
SUM159R
Tumor weight (g)
Vehicle
JQ1
dBET6 qd
dBET6 bid
N
Vehicle
JQ1
dBET6 qd
dBET6 bid
SUM149R
SUM159R
H&E
Ki67

Fig. S4

Figure S5. Related to Figure 5. Chromatin binding patterns of BRD2, BRD4, and BRD7.
(A) BRD4, BRD2 and H3K27ac chromatin binding peaks in promoter and enhancer regions in SUM149 cells. Enhancers were identified based on SUM149 H3K27ac ChIP-seq using the ROSE pipeline.
(B) Changes in BRD4, BRD2, and H3K27ac ChIP-seq chromatin binding peaks between JQ1-treated and untreated SUM149 cells (left panel) and between JQ1-treated resistant SUM149R and parental SUM149 cells (right panel). Outer violin indicates the entire distribution, inner violin (white) indicates the IQR, and ‘‘.’’ and ‘‘+’’ indicate the median and mean, respectively.
(C) Pairwise correlations of changes of BRD4, BRD2, and H3K27ac chromatin binding peaks in promoter and enhancer regions, between treated (+JQ1) and untreated (-JQ1) SUM149 cells (left panel) and between JQ1 treated SUM149R and SUM149 cells (right panel).
(D) Correlation of CTCF binding with BRD2, BRD4, BRD7, and H3K27ac peaks in enhancer and promoter regions.
(E) Correlations of BRD4 chromatin binding peaks in promoter, enhancer, and super-enhancer (SE) regions and their gene expression changes, between treated (+JQ1) and untreated (-JQ1) SUM149 cells and between JQ1 treated SUM149R and SUM149 cells.
(F) Gene tracks depicting BRD4, BRD2, and H3K27ac signal at the *BRD2* and *CCND1* locus. *X*-axis shows position along the chromosome with gene structure below. *Y*-axis shows genomic occupancy in reads per million reads (RPM).
(G) Gene set enrichment analysis (GSEA) depicting the relationship between expression of genes in *BRD7* knockout (KO) cells and JQ1-resistant SUM159R cells, treated with DMSO. Genes are ranked by expression change between SUM159R and SUM159 cells, with upregulated genes in SUM159R cells on the left and downregulated genes in SUM159R cells on the right.
(H) Top process networks enriched in differentially expressed genes between *BRD7* knockout and scramble sgRNA in SUM159 cells. Red and blue indicates upregulated and downregulated pathways, respectively.
(I) Basal, luminal, and mesenchymal signature scores for SUM159 (WT) and SUM159 *BRD7* knockout (KO) cells.
(J) Association between chromatin changes based on ATAC-seq and gene expression changes in two *BRD7* KO clones compared with WT SUM159 cells. Upregulated and downregulated genes are shown in red and blue, respectively.
(K) Heatmap depicting correlation of ATAC-seq peaks between the indicated samples (SUM159 and SUM159R, BRD7 KO and WT cells) treated with DMSO (-) or JQ1 (+).
(L) TEAD motif enriched in ATAC-seq peaks gained in BRD7 KO cells compared to parental SUM159 WT cells associated with genes upregulated in BRD7 KO cells.

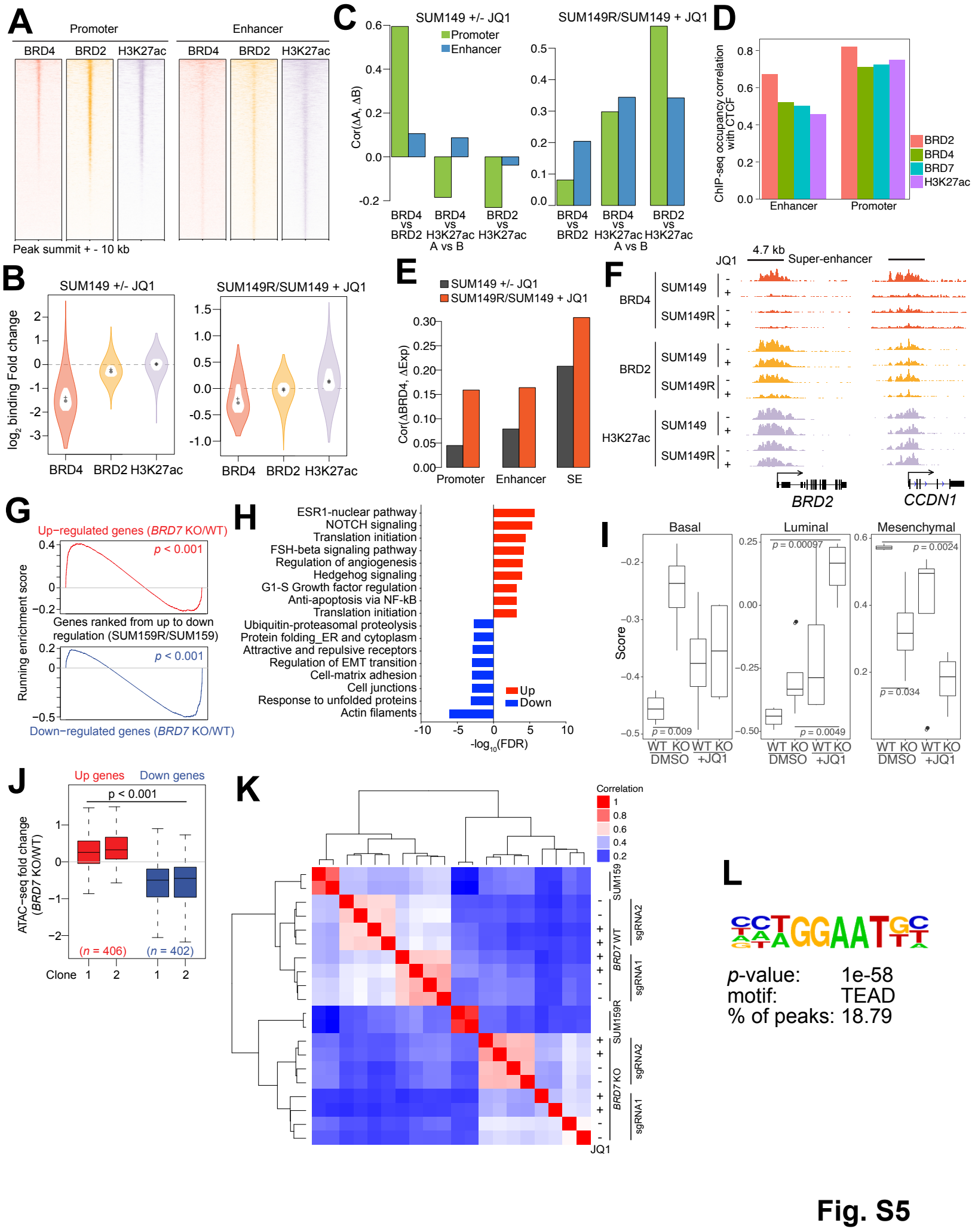
A
Promoter
Enhancer
BRD4
BRD2
H3K27ac
Peak summit + - 10 kb
B
SUM149 +/- JQ1
SUM149R/SUM149 + JQ1
log2 binding Fold change
BRD4 BRD2 H3K27ac
C
SUM149 +/- JQ1
SUM149R/SUM149 + JQ1
Promoter
Enhancer
Cor(ΔA, ΔB)
BRD4 vs BRD2
BRD4 vs H3K27ac
BRD2 vs H3K27ac
A vs B
D
ChIP-seq occupancy correlation with CTCF
BRD2
BRD4
BRD7
H3K27ac
Enhancer
Promoter
E
SUM149 +/- JQ1
SUM149R/SUM149 + JQ1
Cor(ΔBRD4, ΔExp)
Promoter
Enhancer
SE
F
JQ1
4.7 kb
Super-enhancer
BRD4
BRD2
H3K27ac
SUM149
SUM149R
BRD2
CCDN1
G
Up−regulated genes (BRD7 KO/WT)
p < 0.001
Genes ranked from up to down regulation (SUM159R/SUM159)
Running enrichment score
Down−regulated genes (BRD7 KO/WT)
H
ESR1-nuclear pathway
NOTCH signaling
Translation initiation
FSH-beta signaling pathway
Regulation of angiogenesis
Hedgehog signaling
G1-S Growth factor regulation
Anti-apoptosis via NF-kB
Translation initiation
Ubiquitin-proteasomal proteolysis
Protein folding_ER and cytoplasm
Attractive and repulsive receptors
Regulation of EMT transition
Cell-matrix adhesion
Cell junctions
Response to unfolded proteins
Actin filaments
Up
Down
-log10(FDR)
I
Basal
Luminal
Mesenchymal
Score
p = 0.009
p = 0.00097
p = 0.0049
p = 0.0024
p = 0.034
WT KO WT KO
DMSO +JQ1
J
Up genes
Down genes
p < 0.001
ATAC−seq fold change (BRD7 KO/WT)
(n = 406)
(n = 402)
Clone 1 2 1 2
K
Correlation
SUM159
BRD7 WT
BRD7 KO
sgRNA1
sgRNA2
JQ1
L
p-value: 1e-58
motif: TEAD
% of peaks: 18.79

Fig. S5

Figure S6. Related to Figures 5 and 6. Changes in BRD4 chromatin binding and histone modification patterns in BRD7 KO SUM159 cells and crelevance of BRD4 and BRD7 expression in human breast tumor samples.

(A) Heatmap showing the correlation of fold changes in BRD4, H3K27ac, H3K4me3, H3K27me3 ChIP-seq, ATAC-seq, and mRNA expression between BRD7 knockout and scramble control SUM159 cells (top left), and compared to the correlation of fold changes in BRD4 binding upon JQ1-treatment and JQ1-resistance in SUM159 cells (bottom right).

(B) Log2 fold change of ChIP-seq, ATAC-seq and mRNA expression between BRD7 KO/WT in BRD4 binding increased (red) and decreased (blue) peaks in SUM159. The union of BRD7 peaks in SUM159 +/- JQ1 (q<1e-6) were used as anchor. The 1.2 fold change was used to identify an increased or decreased BRD4 binding change. P-values indicate statistical significant by Wilcoxon test.

(C) Line plot showing the smoothed signal of BRD4, H3K27ac, H3K4me3, and H3K27me3 ChIP-seq and ATAC-seq in BRD7 knockout and scramble SUM159 cells at promoters, and comparison to that of BRD4 ChIP-seq signal in DMSO, JQ1-treated and JQ1-resistant SUM159 cells (bottom two tracks). Promoters are ranked by the fold change of BRD4 signal between +/- JQ1 from high (left) to low (right).

(D) Box plots depicting the expression of *BRD4*, *BRD7*, and *ARID1A* in major breast tumor subtypes in the TCGA cohort. Major breast tumor subtypes: basal (n=171), HER2 (n=78), LumA: Luminal A (n=499), LumB: Luminal B (n=197), normal (n=36). Wilcoxon test p values are shown.

(E) Box plots depicting the expression of *BRD4*, *BRD7*, and *ARID1A* in three different subtypes of TNBC in the TCGA cohort. Subtypes of TNBC: basal (n=60), Lum: luminal (n=45), Mes: mesenchymal (n=66). Wilcoxon test p values are shown.

(F) Associations between *BRD4* and *BRD7* expression levels and overall survival among TNBC cases in the TCGA cohort. Patients were divided by the median expression of *BRD4* or *BRD7* across all patients to stratify patients into the low and high groups in the upper panel. The bottom panel shows the clinical associations of the interaction between the two genes. Patients were first divided into low and high *BRD4* groups by the median expression of *BRD4* across all patients; then patients in each group were further divided into two equal sized sub-groups by the median expression of *BRD7* across patients in the corresponding group. The logrank test p values are shown.

(G) Association between *BRD4* and *BRD7* mRNA levels and expression of JQ1 resistance signature (JQ1 resistance score) in TNBC cases in the TCGA cohort. Wilcoxon test p values are shown.

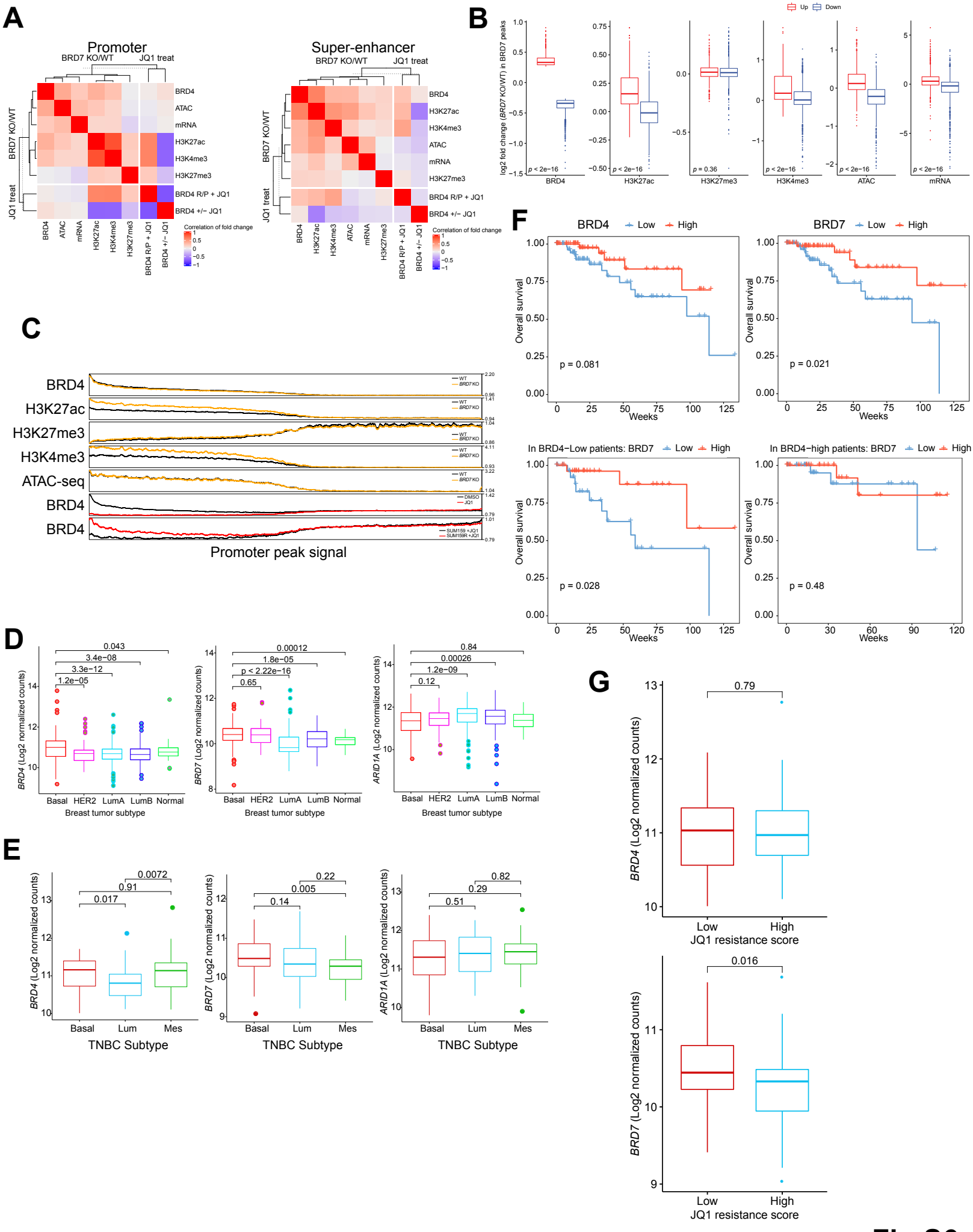
A
Promoter
BRD7 KO/WT
JQ1 treat
BRD4
ATAC
mRNA
H3K27ac
H3K4me3
H3K27me3
BRD4 R/P + JQ1
BRD4 +/− JQ1
Correlation of fold change
Super-enhancer
B
Up
Down
log2 fold change (BRD7 KO/WT) in BRD7 peaks
p < 2e−16
p = 0.36
C
Promoter peak signal
WT
BRD7 KO
DMSO
JQ1
SUM159 +JQ1
SUM159R +JQ1
D
BRD4 (Log2 normalized counts)
BRD7 (Log2 normalized counts)
ARID1A (Log2 normalized counts)
Basal HER2 LumA LumB Normal
Breast tumor subtype
E
Basal Lum Mes
TNBC Subtype
F
Low
High
Overall survival
Weeks
p = 0.081
p = 0.021
In BRD4−Low patients: BRD7
In BRD4−high patients: BRD7
p = 0.028
p = 0.48
G
JQ1 resistance score
Low
High

Fig S6

Figure S7. Related to Figure 7. scRNA-seq data.
(A) *t*-SNE plots depicting relative expression levels of selected genes in single cells of populations indicated in Figure 7A.
(B) Fraction of cells in different phases of cell cycle in each cell line.
(C) Basal, luminal, and mesenchymal signature scores for single cells in SUM149, SUM149R, SUM159, and SUM159R cell lines, with or without JQ1 (left) and indicated clusters in SUM159R cells (right).
(D) Heatmap depicting correlation of ATAC-seq peaks between bulk and scATAC-seq data.
(E) Graph depicts cumulative frequencies of barcodes ranked by abundance in pre-treatment, DMSO, and JQ1-treated SUM149 and SUM159 cells.

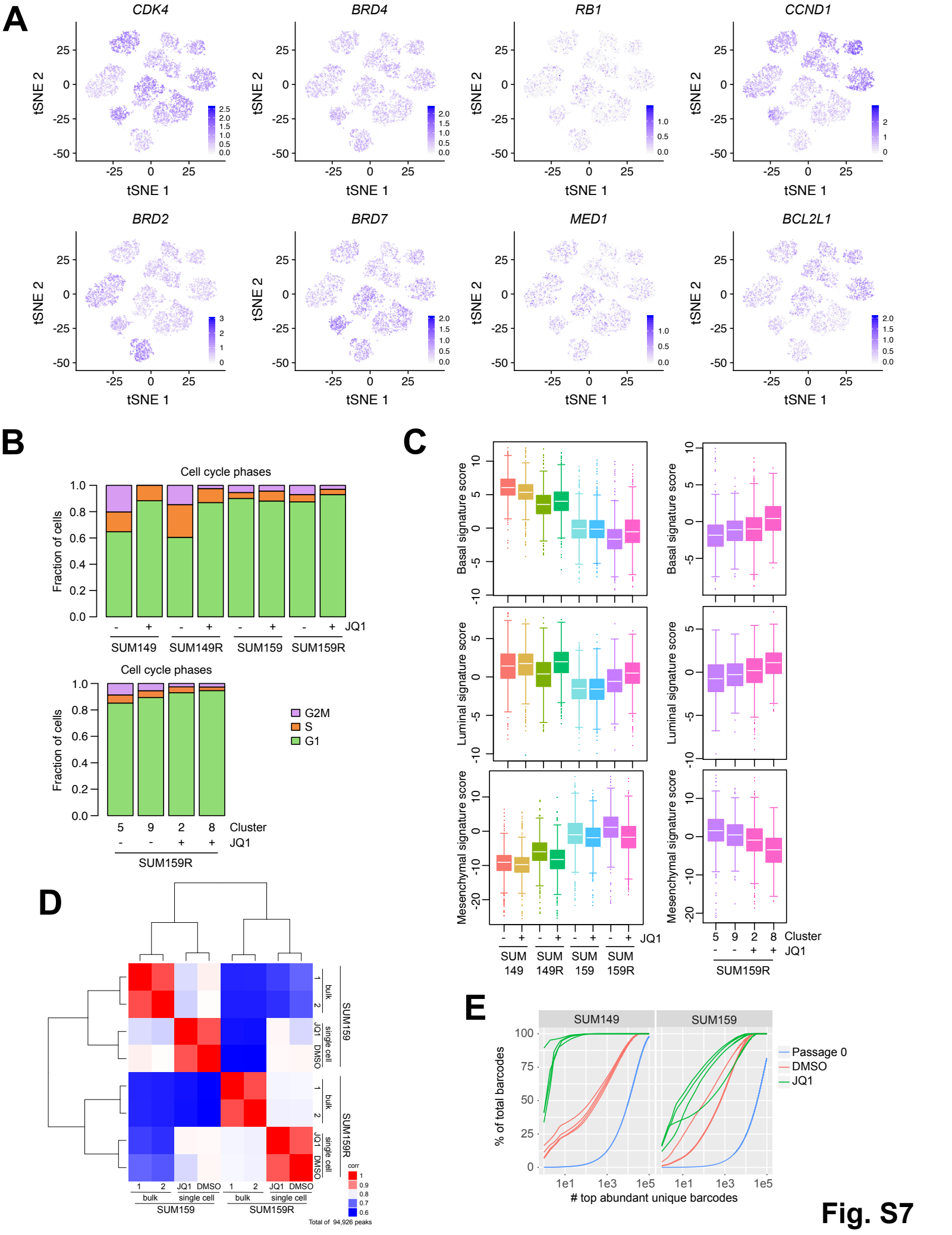
A
CDK4
BRD4
RB1
CCND1
BRD2
BRD7
MED1
BCL2L1
tSNE 1
tSNE 2
B
Cell cycle phases
Fraction of cells
G2M
S
G1
JQ1
SUM149
SUM149R
SUM159
SUM159R
Cluster
C
Basal signature score
Luminal signature score
Mesenchymal signature score
D
bulk
single cell
corr
Total of 94,926 peaks
E
% of total barcodes
# top abundant unique barcodes
Passage 0
DMSO
JQ1

Fig. S7